Assessment of the Hindlimb Membrane Musculature of Bats: Implications for Active Control of the Calcar

KATHRYN E. STANCHAK ⓘ* AND SHARLENE E. SANTANA ⓘ

Department of Biology and Burke Museum of Natural History and Culture, University of Washington, Seattle, Washington

ABSTRACT

The striking postcranial anatomy of bats reflects their specialized ecology; they are the only mammals capable of powered flight. Bat postcranial adaptations include a series of membranes that connect highly-modified, or even novel, skeletal elements. While most studies of bat postcranial anatomy have focused on their wings, bat hindlimbs also contain many derived and functionally important, yet less studied, features. In this study, we investigate variation in the membrane and limb musculature associated with the calcar, a neomorphic skeletal structure found in the hindlimbs of most bats. We use diffusible iodine-based contrast-enhanced computed tomography and standard histological techniques to examine the calcars and hindlimb membranes of three bat species that vary ecologically (*Myotis californicus*, a slow-flying insectivore; *Molossus molossus*, a fast-flying insectivore; and *Artibeus jamaicensis*, a slow-flying frugivore). We also assess the level of mineralization of the calcar at muscle attachment sites to better understand how muscle contraction may enable calcar function. We found that the arrangement of the calcar musculature varies among the three bat species, as does the pattern of mineral content within the calcar. *M. molossus* and *M. californicus* exhibit more complex calcar and calcar musculature morphologies than *A. jamaicensis*, and the degree of calcar mineralization decreases toward the tip of the calcar in all species. These results are consistent with the idea that the calcar may have a functional role in flight maneuverability. Anat Rec, 301:441–448, 2018. © 2018 Wiley Periodicals, Inc.

Key words: muscle; adaptation; Chiroptera; neomorphism

The evolution of flight and associated morphologies in bats (Chiroptera) is an example of how anatomical evolution can enable new functional abilities and lead to ecological diversification (Simmons, 2005; Teeling et al., 2005). Once bats evolved a highly-modified postcranial skeleton and a series of membranes (patagia) that enabled powered flight (Fig. 1), they radiated to fill numerous ecological niches and evolved corresponding morphological and functional specializations (Norberg and Rayner, 1987). For instance, the shape of wing membranes varies among bats, corresponding with different flight ecologies among species (Norberg and Rayner, 1987). Furthermore, bat membranes contain musculature, associated nerves, and elastin fibers that vary across species and are hypothesized to contribute to the mechanical properties of the membrane and to active and passive control of membrane shape during flight (Holbrook and Odlund, 1978; Swartz et al., 1996; Cheney et al., 2014a, 2017).
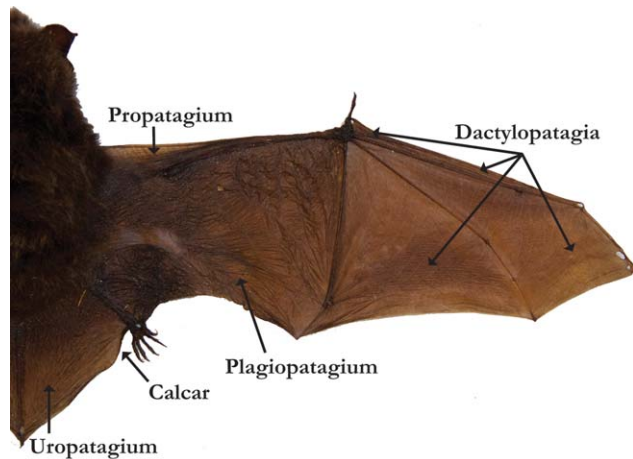
Fig. 1. Extended wing of *Myotis* sp. demonstrating the series of patagia that form the bat wing and the location of the calcar.

Postcranial studies of bats have primarily focused on the forewing (e.g., wing membranes: Cheney et al., 2014a,; wing bones: Swartz et al., 1992; forelimb development: Sears et al., 2006). However, bat hindlimbs are also highly modified and presumably specialized for many tasks, including prey capture and hanging, as well as flight (Fish et al., 1991; Simmons and Quinn, 1994; Cheney et al., 2014b). Because bats are ecologically diverse, the functional requirements of these tasks vary widely among species. As such, the primary evolutionary pressures on hindlimb morphology likely differ among species, leading to functionally relevant variation. Supporting this idea, the shape and size of the uropatagium vary considerably among bat species (Hill and Smith, 1984; Schutt and Simmons, 1998). Furthermore, bats have evolved a calcar, a neomorphic (Hall, 2005) spur of cartilage that arises from the bat ankle, articulates with the calcaneus tarsal, and extends into the posterior margin of the uropatagium (Fig. 1). The calcar suddenly appears in the oldest known bat postcrania (*Onychonycteris finneyi*, ca. 52.5 Ma, Simmons et al., 2008) and is found in a large majority of bat species, although it has been lost in some (Schutt and Simmons, 1998). Analogous but not homologous structures are known from other tetrapod lineages, including the styliform cartilages of gliding rodents, the pteroid of pterosaurs, and the styliform element of the membrane-bound maniraptor *Yi qi* (Xu et al., 2015). Because the calcar is found throughout a speciose and diverse clade (Chiroptera), it provides a unique opportunity to study morphological and functional diversity in newly-evolved skeletal elements.

Little is known about the function of the calcar and its associated musculature, as there are few detailed anatomical studies of these structures. Schutt and Simmons (1998) presented a broad overview of the calcar and associated musculature across all bat families. These descriptions built upon previous work by Humphry (1869), MacAlister (1872), Maisonneuve (1878), Morra (1899), de Fénis (1919), Vaughan (1959, 1970a), Mori (1960), and Grassé (1971). (For a full review, see Schutt and Simmons, 1998). In all bats that had a calcar, they found two muscles that attach to the calcar: the m. calcaneocutaneous and the m. depressor ossis styliformis. They depicted the m. calcaneocutaneous as originating from the anterior margin of the calcar and inserting onto the medial raphe of the uropatagium posterior to the tail. As tail length varies among bat species, often extending to the posterior margin of the uropatagium, the insertion of the m. calcaneocutaneous is variable. The m. depressor ossis styliformis originates from the fifth metatarsal and the medial surface of the calcaneus and inserts onto the posterior margin of the calcar. Schutt and Simmons (1998) also noted that the calcar is present in both mineralized and unmineralized forms in different species of bats, and they suggested that variation in calcar and uropatagium shape, size, and structure has implications for dietary and foraging strategies.

In the present study, our goal is to better understand the anatomy of the uropatagial musculature associated with the calcar, its variation among species, and its possible function. We expand upon previous descriptions of bat uropatagial anatomy by detailing interspecific differences in the musculature that controls the calcar among three distantly-related bat species that vary morphologically and ecologically: (1) *Myotis californicus* (Vespertilionidae), an aerial insectivore with relatively slow flight; (2) *Molossus molossus* (Molossidae), an aerial insectivore with fast flight; and (3) *Artibeus jamaicensis* (Phyllostomidae), a frugivore that forages within the cluttered forest (Norberg and Rayner, 1987). Aerial insectivores like *M. californicus* capture small, agile prey during flight and thus must be able to change directions quickly. Molossid bats like *M. molossus* are also aerial insectivores, but they are morphologically adapted to reduce drag and fly fast over long distances and are consequently less maneuverable over short distances (Vaughan, 1970b). Both of these species use their uropatagium to aid in prey capture. Conversely, frugivores capture and feed on stationary targets; *A. jamaicensis* grabs fruits with its mouth and consumes them while hanging (rather than consuming the fruits while hovering like nectarivorous bats). Due to these differences in requirements for maneuverable flight, it has been suggested that frugivores possess a less specialized flight apparatus (Vaughan, 1970b). Here, we test the hypothesis that the morphology of the calcar and associated musculature will vary among *M. californicus*, *M. molossus*, and *A. jamaicensis* due to the different functional requirements of their flight patterns. We expect that species that require higher flight maneuverability and/or flight speeds (aerial insectivores) will exhibit a more complex calcar muscle arrangement that allows for finer control of calcar motion, whereas the less maneuverable frugivore will exhibit a simpler calcar muscle arrangement.

MATERIALS AND METHODS
DiceCT and Virtual Dissections

We used diffusible iodine-based contrast-enhanced computed tomography (diceCT; Gignac et al., 2016) to assess calcar musculature anatomy, as this method allowed us to study the morphology of soft tissue elements without causing permanent damage to the original specimens. We dissected one hindlimb from one specimen each of *M. californicus, M. molossus*, and *A. jamaicensis*. These specimens had previously been preserved in 10% neutral-buffered formalin (NBF) and then stored in 70% ethanol.

We placed each hindlimb into a 3% wt/vol Lugol's iodine solution (1% wt/vol I_2, 2% wt/vol KI). Because the bats varied in size, they required different staining times in the iodine solution: *M. californicus*, 2 days; *M. molossus*, 3 days; *A. jamaicensis*, 4 days. We scanned each specimen in a Skyscan 1172 μCT scanner (Bruker MicroCT, Belgium) at 40 kV and 201 μA with a 0.5 mm aluminum filter at a resolution of 11.76 μm. We also scanned a separate iodine-stained specimen of *M. californicus* at a higher resolution (6.34 μm) to better distinguish features during the virtual dissection. To ensure that the uropatagia remained in an extended position during the scan, we sewed each hindlimb with the membrane extended to a piece of styrofoam. We reconstructed our X-ray projections from the μCT scans using NRecon software (Bruker MicroCT, Belgium) and viewed our reconstructed scans using CTvox (Bruker MicroCT, Belgium), a volume-rendering software that allows for 3D visualization of CT scans. We used DataViewer (Bruker MicroCT, Belgium) to measure the length of the tibia of each bat as a scale for the CTvox images. We then imported our reconstructed scans into Mimics 18.0 (Materialize, Ann Arbor, MI) and digitally dissected the calcar, the m. depressor ossis styliformis, and adjacent anatomical features. We also used Mimics 18.0 to measure the total calcar length of each specimen.

Conventional CT Scanning and Mineralization Observations

To better assess the functional implications of variation in calcar musculature anatomy and to support our diceCT results, we also μCT scanned one hindlimb from different specimens of each of the target species (Skyscan 1172; 50–60 kV and 167–201 μA with a 0.5 mm aluminum filter). To evaluate calcar mineralization, we scanned these specimens with 0.25 and 0.75 calcium hydroxyapatite (CaHA) standards (Bruker MicroCT, Belgium). The specimens used had been fixed in 10% NBF for variable periods of time prior to storage in 70% ethanol. Because formalin is a mild decalcifier, any quantitative results based on this method are inaccurate; rather, our intent was to use both the diceCT and conventional CT scans to qualitatively assess mineral content within each scan to determine which portions of the calcar were calcified or uncalcified.

Histology

After diceCT scanning, we leached the iodine from the hindlimbs by placing them in several washes of 70% ethanol over the course of one week. To speed the leaching process, we placed the specimens in their leaching solution in a 37°C shaker. We then dissected the hindlimbs into uropatagium and calcar/depressor muscle pieces. With the help of the volume-rendered CTvox images, we attempted to dissect these pieces such that we could obtain cross-sections of the m. depressor ossis styliformis perpendicular to the longitudinal plane of the calcar, and sections of the m. calcaneocutaneous in the plane perpendicular to the muscle fiber orientation. We placed all mineralized pieces of tissue (*M. molossus* and *M. californicus* calcars) in a 12% EDTA solution in a 37°C shaker for one week to decalcify. To prepare for histological sectioning, we dehydrated all tissue pieces through a series of increasing

ethanol concentrations, cleared them in xylene, and infiltrated them with paraffin wax. We then embedded each piece in a paraffin block, cut the block into 6 μm sections on a Leica RM2145 microtome, and cleared and rehydrated each section. We stained the sections with Modified Mayer's Hematoxylin followed by a Mallory triple connective tissue stain (Humason, 1962). We briefly soaked each section in 1% acetic acid before dehydrating them through the alcohol series, clearing them with xylene, and mounting them with a xylene–toluene resin and coverslip. We imaged the sections with a Nikon Eclipse E600FN compound microscope and an AmScope MU300 microscope-mounted camera.

RESULTS

Gross Anatomy of Calcar Musculature

M. californicus—The uropatagial muscles are composed of distinct, separate bundles of fibers (Fig. 2a). The CTvox rendering of the diceCT scan appears to show one bundle near the ankle joint originating from the calcar itself (the m. calcaneocutaneous), although small folds in the membrane made this difficult to discern. The remainder of the bundles originate from the tibia, forming the m. tibiocutaneous. We did not see attachment of the m. calcaneocutaneous to the calcar in any histological sections. Virtual dissection from the diceCT scan revealed that the m. depressor ossis styliformis of *M. californicus* originates from both the calcaneus and the cuboid and inserts onto the posterior margin of the calcar (Fig. 3a). The diceCT scan also revealed an uncalcified spur on the posterior margin of the calcar, onto which the medial edge of the m. depressor ossis styliformis appears to insert (Figs. 3a and 4a).

M. molossus—The m. calcaneocutaneous is a flat sheet of fibers along the dorsal side of the uropatagium that originates from the anterior margin of the calcar. These are not immediately recognizable in the CTvox rendering of the diceCT scan, but they are visible in histological sections (Figs. 2b and 4c,d). The m. depressor ossis styliformis consists of two separate muscle compartments. The first, which we call the m. depressor ossis styliformis profundus, originates from the calcaneus and inserts onto the portion of the calcar proximal to the ankle, wrapping around the posterior margin. The second, the m. depressor ossis styliformis superficialis, originates from the 5th metatarsal, runs beneath the m. depressor ossis styliformis profundus and inserts distally along the calcar, closer to the tail and the midline of the uropatagium (Figs. 3b and 4c,d). We also noticed an additional muscle that runs beneath the m. depressor ossis styliformis (Fig. 4c). This additional muscle extends medially to a sheath of muscle surrounding the tail, but its origination and insertion are unclear from the diceCT scans. It was not found in the other two species.

A. jamaicensis—Of the three bats examined, the calcar musculature of *A. jamaicensis* best conforms to previous descriptions (Schutt and Simmons, 1998). The m. calcaneocutaneous is a relatively thick, flat sheet of regularly-arranged fibers originating from the anterior margin of the calcar (Figs. 2c and 4b). The m. depressor ossis styliformis originates from the fifth metatarsal and inserts onto the posterior margin of the calcar (Figs. 3c and 4b). The calcar of *A. jamaicensis* is relatively shorter than those of the other two bats, and the m. depressor
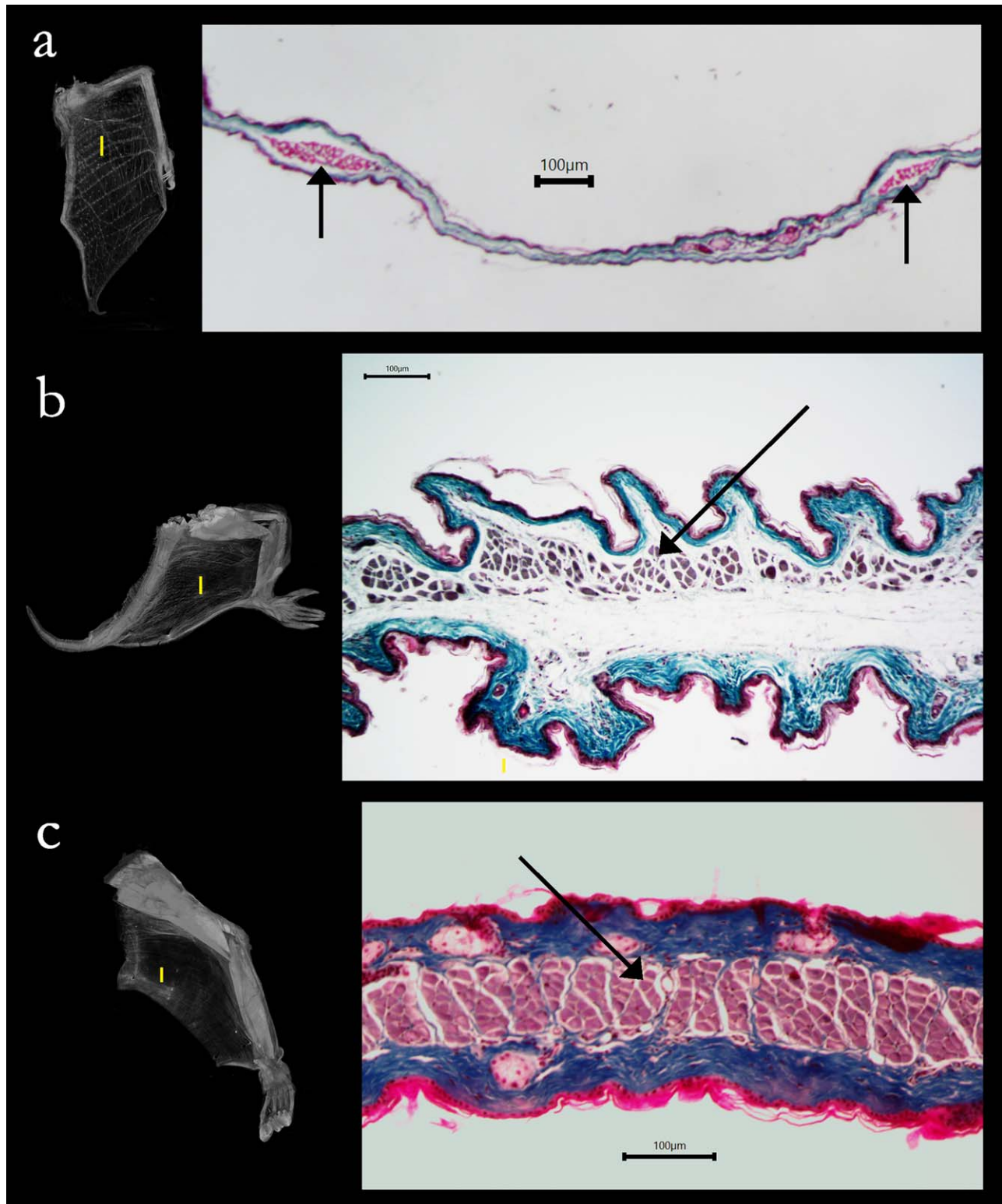
Fig. 2. Mallory-stained histological sections through the uropatagia of (**a**) *M. californicus*, (**b**) *M. molossus*, and (c) *A. jamaicensis*. The dorsal side of each section is on the upper half of the image. Arrows point to the uropatagial cutaneous muscles [m. tibiocutaneous in (a); m. calcaneo-cutaneous in (b,c)]. Scale bars on the histological sections are 100 μm. Insets for each image indicate the approximate location of each section on the volume-rendered diceCT scan of each specimen. For comparing relative size, the tibia lengths for each specimen are (a) 12.4 mm, (b) 14.4 mm, and (c) 19.5 mm.
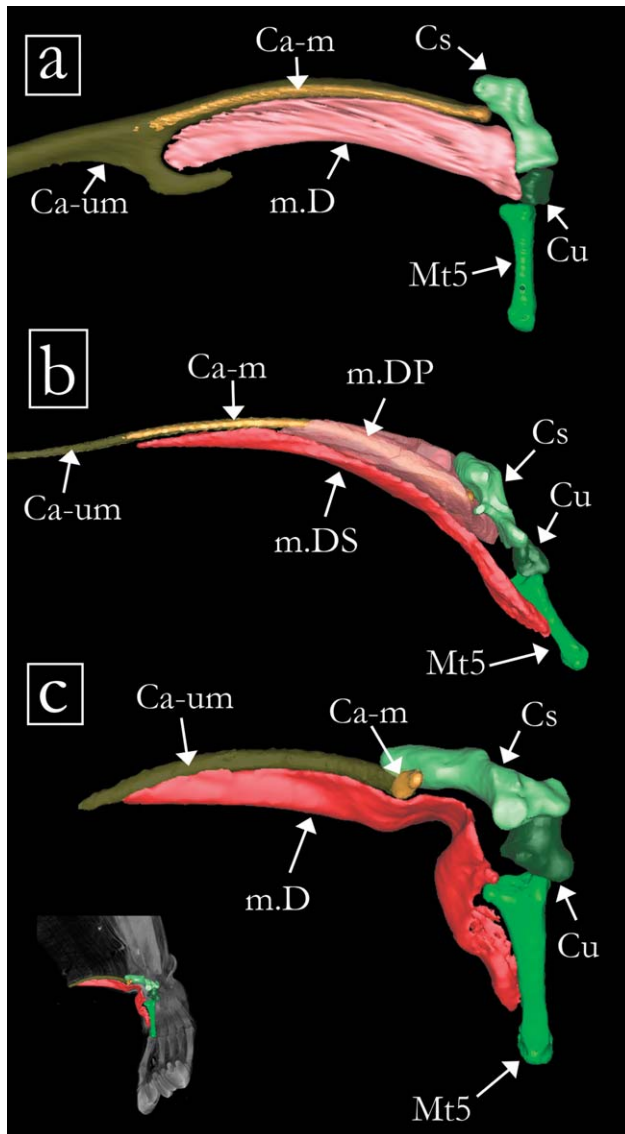
Fig. 3. Virtual dissections in ventral view of the calcar-depressor muscle complex of one hindlimb each of (**a**) *M. californicus*, (b) *M. molossus*, and (c) *A. jamaicensis*. The inset illustrates the location of the dissection models using the *A. jamaicensis* volume-rendered diceCT scan. The tips of the calcars of *M. californicus* and *M. molossus* are cropped to better view the ankle region. Ca-m, mineralized calcar; Ca-um, unmineralized calcar; Cs, calcaneus; Cu, cuboid; m.D, m. depressor ossis styliformis; m.DP, m. depressor ossis styliformis profundus; m.DS, m. depressor ossis styliformis superficialis; Mt5, fifth metatarsal.

ossis styliformis runs almost the entire length of the calcar, rather than only inserting on the half proximal to the ankle.

Calcar Length and Mineralization

Both the conventional CT and the diceCT scans revealed notable differences in calcar length among the three bat species (see CTvox renderings of diceCT scans in Fig. 2). In *M. californicus*, the calcar spans ∼50% of the distance between the ankle and the tail (13.6 mm),

leaving the posterior edge of the uropatagium closest to the tail unsupported. In *M. molossus*, the calcar tapers to a thin band ∼70% of the distance between the ankle and the tail (12.9 mm). We were unable to follow the full length of this band in the diceCT scan to determine if it is connected to the tail or the sheath of muscle surrounding the tail. In *A. jamaicensis*, the calcar extends to the medial edge of the uropatagium and is relatively shorter than those of the other two bats examined (3.2 mm), possibly because this species has a reduced uropatagium (Fig. 2c).

Both the conventional and the diceCT scans of iodine-stained bat hindlimbs showed variable pixel intensity within the calcar of each individual bat, indicating variation in mineralization along the length of the calcar. The calcars of *M. californicus* and *M. molossus*, in particular, are more mineralized near the ankle and unmineralized closer to the tail (Fig. 3). In both of these species, the length of the mineralized portion corresponds with the insertions of the m. depressor ossis styliformis. The calcar of *A. jamaicensis* exhibits a small, calcified nodule near the joint with the calcaneus, but is largely unmineralized, even along the insertion of the m. depressor ossis styliformis.

DISCUSSION
Functional Implications of Interspecific Variation in Uropatagium and Calcar Musculature

The hindlimb membrane apparatus of bats underwent great morphological diversification as the lineage radiated to fill different ecological niches. The presence of muscles that originate from and insert onto the calcar and the observed variation in the arrangement of these muscles among species likely reflect functional aspects of ecological diversification. Our results suggest that bats vary in the amount of control they have over the motion of the calcar and thus, the shape of the uropatagium, and that this variation may correspond with different flight ecologies.

The presence of two distinct depressor muscles that insert onto the calcar of *M. molossus* is a remarkable finding that indicates that this bat has independent control over the portion of the calcar closer to the ankle and the portion more distal from the ankle. This would give *M. molossus* fine control over the expansion and shape of the uropatagium. In contrast, *A. jamaicensis* and *M. californicus* have only one muscle that depresses the calcar. The m. depressor ossis styliformis of *M. californicus*, however, inserts onto both the main body of the calcar and onto a cartilaginous spur of the calcar that projects into the posterior margin of the uropatagium. Consequently, a contraction of the m. depressor ossis styliformis in *M. californicus* would serve to spread the uropatagium in posterior and lateral directions simultaneously. Thus, the presence of two distinct depressor muscles in *M. molossus* and a cartilaginous calcar spur in *M. californicus* may be two different solutions to enhance control of the uropatagium as these species pursue and capture fast insect prey. While maneuverability is also important for *A. jamaicensis* as it navigates cluttered forest habitat, the agility required to avoid tree branches and locate fruits may present less of a
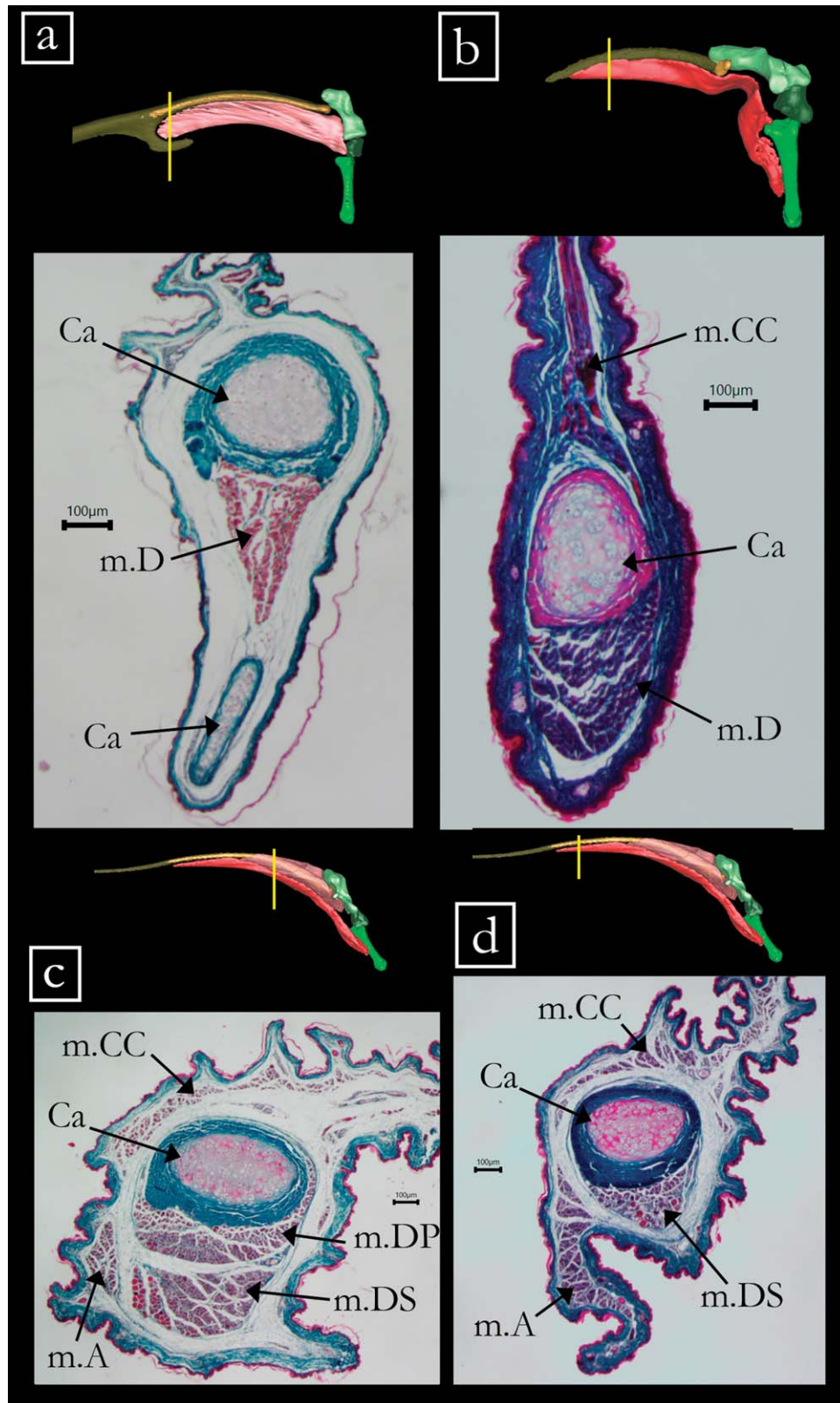
Fig. 4. Mallory-stained histological sections through the calcar of (**a**) *M. californicus*, (**b**) *A. jamaicensis*, and (**c,d**) *M. molossus*. The anterior side of each section is on the upper half of the image. Insets for each image indicate the approximate location of each section on the volume-rendered diceCT scan of each specimen. Scale bars are 100 μm. Ca, calcar; m.A, additional muscle in *M. molossus*; m.CC, m. calcaneocutaneous; m.D, m. depressor ossis styliformis; m. DP, m. depressor ossis styliformis profundus; m.DS, m. depressor ossis styliformis superficialis.

functional challenge than that required to catch flying insects (Vaughan, 1970b). Flight agility and maneuverability have been experimentally compared between insectivorous species of bats (Aldridge, 1986; Aldridge et al., 1987) and between frugivores (Stockwell, 2001), but additional studies comparing the same agility and maneuverability patterns among bats of different ecologies and with different flight patterns are required to further support this idea.

The m. calcaneocutaneous also varies among the three bat species we examined. First, the fibers of the sheet-like m. calcaneocutaneous are more sparsely distributed in *M. molossus* than in *A. jamaicensis*. *M. molossus* has a unique sheath of muscle surrounding its tail vertebrae. This muscle might actuate the retraction of the uropatagium along the tail either to free the hindlimbs as the bat moves quadrupedally in crevices or to reduce drag during flight (Vaughan, 1966). Thus, the m. calcaneocutaneous may play less of a role in controlling the uropatagium than the tail sheath in *M. molossus*. It is also possible that the elastic properties of the muscle fibers of the m. calcaneocutaneous serve to passively counter the action of the m. depressor ossis styliformis in either of these species, for example by tightening the membrane to reduce flutter during flight. Second, most if not all of the membrane muscle bundles in *M. californicus* form the m. tibiocutaneous (Schutt and Simmons, 1998) rather than the m. calaneocutaneous. This suggests that *M. californicus* has limited control of its calcar from producing anterior (elevator) forces. Even if one or more muscle bundles do originate from the ankle joint, the total cross-sectional area of the muscle would be quite small, and any force produced would be near the pivot point of the joint, generating little torque. This indicates that there is no or very little antagonistic torque to counter the m. depressor ossis styliformis in *M. californicus*.

Calcar Length, Mineralization, and Muscle Attachments

The length of the calcar, and the extent to which it spans and supports the posterior margin of the uropatagium, varies considerably among the three species studied. In *M. californicus*, the edge of the uropatagium closest to the tail is unsupported by the calcar, resulting in a trailing edge that is free to flutter unless stretched by the surrounding skeleton and musculature. The calcar of *M. molossus* also does not extend fully to the tail, but the additional, undescribed muscle we found may provide some stiffness to the posterior margin of the uropatagium closest to the tail.

Our CT scans revealed variation in mineral content along individual calcars, which indicates that material properties also vary along calcars. This has implications for the response of the calcar to the force produced by the contractions of the muscles that insert onto it. A contraction of the m. inferior ossis styliformis may cause an uncalcified or little-calcified calcar to bend rather than (or as well as) rotate about its articulation with the calcaneus. This additional source of calcar variation might give bats finer control over the extent to which their uropatagium is spread, thus helping them change the amount of lift produced and drag experienced during flight.

Future Work and Conclusions

Our anatomical findings have led to several hypotheses about the function and physiology of the uropatagium and calcar muscles. To test these, future work should examine the innervation of these muscles, as well as test biomechanical models of the calcar apparatus. Tokita et al. (2012) used a developmental approach to study the innervation of wing membrane muscles in two vespertilionid species. They discovered that the m. calcaneocutaneous (called the m. uropataginalis in their study) is primarily innervated by a branch of the lumbar and sacral plexuses that corresponds to a branch innervating the semitendinosus. However, they did not provide detailed information on the innervation of each bundle of fibers nor on the innervation of the m. depressor ossis styliformis. Our results indicate that it is particularly important to determine the innervation of the depressor muscle complex in *M. molossus* to test our hypothesis that the m. depressors ossis styliformis profundus and superficialis can contract independently.

We have presented only qualitative descriptions of the muscles associated with the calcar and of calcar mineral content to explore functional variation of the calcar apparatus. To fully understand the implications of calcar anatomical variation to flight performance, future research should build proper quantitative biomechanical models that account for the force of muscle contraction and the bending resistance of the calcar (including measurements of elastic moduli and cross-sectional shape). As the bat calcar is a neomorphic structure that takes on diverse anatomical configurations among bats species, these kinds of studies may serve to improve our understanding of morphological novelty and diversification in the vertebrate skeleton.

ACKNOWLEDGEMENTS

LITERATURE CITED

Aldridge H. 1986. Manoeuvrability and ecological segregation in the little brown (*Myotis lucifugus*) and Yuma (*M. yumanensis*) bats (Chiroptera: Vespertilionidae). Can J Zool 64:1878–1882.

Aldridge HD, Rautenbach JH, Rautenbach IL. 1987. Morphology, echolocation and resource partitioning in insectivorous bats. J Anim Ecol 56:763–778.

Cheney JA, Konow N, Middleton KM, Breuer KS, Roberts TJ, Giblin EL, Swartz SM. 2014a. Membrane muscle function in the compliant wings of bats. Bioinspir Biomim 9:025007.

Cheney JA, Ton D, Konow N, Riskin DK, Breuer KS, Swartz SM. 2014b. Hindlimb motion during steady flight of the lesser dog-nosed fruit bat, *Cynopterus brachyotis*. PLoS One 9:e98093.

Cheney JA, Allen JJ, Swartz SM. 2017. Diversity in the organization of elastin bundles and intramembranous muscles in bat wings. J Anat 230:510–523.

de Fénis F. 1919. Le membre pelvien des Chiroptères. Ses caractères d'adaptation a la suspension, Thèses pour obtenir le grade

de Docteur des Sciences Naturelles, L'Uinversité de Paris. 823, d'ordre 1619.

Fish FE, Blood BR, Clark BD. 1991. Hydrodynamics of the feet of fish-catching bats: influence of the water surface on drag and morphological design. J Exp Zool 258:164–173.

Gignac PM, Kley NJ, Clarke JA, Colbert MW, Morhardt AC, Cerio D, Cost IN, Cox PG, Daza JD, Early CM, et al. 2016. Diffusible iodine-based contrast-enhanced computed tomography (diceCT): an emerging tool for rapid, high-resolution, 3-D imaging of metazoan soft tissues. J Anat 228:889–909.

Grassé PP. 1971. Muscles de la jambe et du pied—Les Chauves-souris. In: Grassé PP, editor. Traité de Zoologie Tome 17. Paris: Maison et Cie. p 386–391.

Hall BK. 2005. Bones and Cartilage: developmental and evolutionary skeletal biology. Academic Press.

Hill JE, Smith JD. 1984. Bats: a natural history. London: British Museum (Natural History).

Holbrook KA, Odland GF. 1978. A collagen and elastic network in the wing of the bat. J Anat 126:21–36.

Humason GL. 1962. Animal tissue techniques. 2nd ed. San Francisco: W.H. Freeman & Co.

Humphry GM. 1869. The myology of the limbs of Pteropus. J Anat Physiol 3:294–491.

MacAlister A. 1872. The myology of the cheiroptera. Philos Trans R Soc Lond B Biol Sci 162:125–171.

Maisonneuve P. 1878. Traité de l'ostéologie et de la myologie du Vespertilio murinus, précédé d'un exposé de la classification des chéiroptères et de considérations sur les moeurs de ces animaux. Paris: Ed: Doin.

Mori M. 1960. Muskulatur des Pteropus edulis. Okajimas Folia Anat Jpn 36:253–307.

Morra T. 1899. I muscoli cutanei della membrana alare dei chirotteri. Bull Mus Zool Ed Anat Comp R. Univ Di Torino XIV, 1–7.

Norberg UM, Rayner JMV. 1987. Ecological morphology and flight in bats (Mammalia; Chiroptera): wing adaptations, flight performance, foraging strategy and echolocation. Philos Trans R Soc Lond B Biol Sci 316:335–427.

Schutt WA Jr, Simmons NB. 1998. Morphology and homology of the Chiropteran calcar, with comments on the phylogenetic relationships of Archaeopteropus. J Mamm Evol 5:1–32.

Sears KE, Behringer RR, Rasweiler JJ, Niswander LA. 2006. Development of bat flight: morphologic and molecular evolution of bat wing digits. Proc Natl Acad Sci USA 103:6581–6586.

Simmons NB. 2005. Order Chiroptera. In: Wilson DE, Reeder DM, editors. Mammal species of the world: a taxonomic and geographic reference. Baltimore, MD: Johns Hopkins University Press. p 312–529.

Simmons NB, Quinn TH. 1994. Evolution of the digital tendon-locking mechanism in bats and dermopterans: a phylogenetic perspective. J Mamm Evol 2:213–254.

Simmons NB, Seymour KL, Habersetzer J, Gunnell GF. 2008. Primitive Early Eocene bat from Wyoming and the evolution of flight and echolocation. Nature 451:818–821.

Stockwell EF. 2001. Morphology and flight manoveurability in New World leaf-nosed bats (Chiroptera: Phyllostomidae). J Zool 254:505–514.

Swartz SM, Bennett MB, Carrier DR. 1992. Wing bone stresses in free flying bats and the evolution of skeletal design for flight. Nature 359:726–729.

Swartz SM, Groves MS, Kim HD, Walsh WR. 1996. Mechanical properties of bat wing membrane skin. J Zool 239:357–378.

Teeling EC, Springer MS, Madsen O, Bates P, O'brien SJ, Murphy WJ. 2005. A molecular phylogeny for bats illuminates biogeography and the fossil record. Science 307:580–584.

Tokita M, Abe T, Suzuki K. 2012. The developmental basis of bat wing muscle. Nat Commun 3:1302.

Vaughan TA. 1959. Functional morphology of three bats: Eumops, Myotis, Macrotus. Univ. Kansas Publ Mus Nat Hist 12:1–153.

Vaughan TA. 1966. Morphology and flight characteristics of Molossid bats. J Mamm 47:249–260.

Vaughan TA. 1970a. The muscular system. In: Wimsatt WA, editor. Biology of bats Vol. 1. New York: Academic Press. p 139–194.

Vaughan TA. 1970b. Flight patterns and aerodynamics. In: Wimsatt WA, editor. Biology of bats. Vol. 1. New York: Academic Press. p 195–216.

Xu X, Zheng X, Sullivan C, Wang X, Xing L, Wang Y, Zhang X, O'Connor JK, Zhang F, Pan Y. 2015. A bizarre Jurassic maniraptoran theropod with preserved evidence of membranous wings. Nature 455:1105–1108.